

## 10.1 Introduction

Evidences from past earthquakes clearly exhibit that the damages due to an earthquake and its severity are controlled mainly by earthquake source and path characteristics along with the site specific issues (Nath *et al.*, 2002; Nath and Thingbaijam, 2011b; Phillips and Hashash, 2009; Hashash and Park, 2002; Aki, 1993; Phillips and Aki, 1986; Su *et al.*, 1992; Kato *et al.*, 1995; Bonilla *et al.*, 1997). This makes site specific seismic response analysis mandatory. With a view to characterize site conditions in the City extensive geophysical and geotechnical investigations have been carried out at 1957 locations encompassing the urban cluster of 435 km<sup>2</sup> of Kolkata (described in greater details in Chapters 5 and 6) with an a priori in-depth information on Geology and Geomorphology of the terrain (discussed and illustrated in Chapter 2). The insitu information of the terrain acquired through both the invasive and non-invasive investigations exhibit low SPT-N values ranging between 1 and 5 for the first 10 m depth substratum adhering to shear wave velocities in the range of 90-150 m/s followed by sediment strata with blow counts less than 19 for the next 20 m stratification with shear wave velocity near about 220 m/s. The SPT-N values and shear wave velocities ranges from 19 to 25 and 220-275 m/s respectively for the depth range of 20-30 m. However, stiff to very stiff sediments with blow count greater than 25 and higher shear wave velocities (>275 m/s) have been encountered beyond 30 m depth. The drilled lithologs and recovered cores indicate the presence of interbedded layers of both cohesive and cohesionless soil in the substratum underlying the City. Cohesive soils are either low plastic silty clays/clayey silt or very high plastic silty clay associated with peat/decomposed wood. The cohesionless soils on the other hand comprise mostly of silty, clayey sands, non-plastic silt and occasional gravels beyond a depth of 40 m. The presence of loose to medium dense coarse grained sediment layers in conjunction with shallow water table makes the subsurface conditions susceptible to soil liquefaction (Kramer, 1996; Nath, 2011). A detailed Pre- and Post-monsoon ground water table fluctuation mapping with data from Piezometers and Dug Wells exhibits water table variation within 0.5-7.7 m for the City (details in Chapter 7) which has direct implications on soil liquefaction hazard assessment (details in Chapter 9). On the other hand, the effective shear wave velocity for 30 m soil column ( $V_s^{30}$ ) estimated from both the insitu measurements and the surface geophysical investigations have been used to perform the site classification of the terrain adhering to NEHRP and Sun (2004) nomenclature that divides the City into five classes D1, D2, D3, D4 and E with the dominance of site classes corresponding to low  $V_s^{30}$  adhering to site classes D4 &

E (details in Chapter 6). The subsurface condition of the City is, therefore, prone to geohazard regime favoring seismic vulnerability. It is felt essential to undertake in-depth site characterization of the City using all the hazard proxies *viz.* site effect, soil liquefaction, fundamental frequency distribution of the basin, geomorphological attribution and site/sediment classification.

## 10.2 Site Amplification

The amplification of ground motion over soft sediments occurs fundamentally due to the impedance contrast between sediments and the underlying bedrock resulting in trapping of seismic waves causing reverberation and scattering of the incident energy (Nath and Thingbaijam, 2009). Therefore, the assessment of site amplification factor for a region located over soft sediments is crucial to account for the changes in ground motion at the surface as compared to that at the engineering bedrock due to the nonlinear behavior of the in-between sediment column and also from site to site on the surface of the earth. In the present analysis, to quantify the effect of sediment layer properties on propagated ground motions, one dimensional equivalent-linear/nonlinear approach for site response analysis proposed by Idriss and Seed (1968) has been adopted and the computation has been performed by using DEEPSOIL (Hashash *et al.*, 2011) software that facilitates both equivalent-linear and nonlinear analyses in the frequency domain and uses the geotechnical parameters *viz.* soil type, thickness of the layer, unit weight of the material, shear wave velocity of the material along with the acceleration time history at the engineering bedrock level as inputs. The assumptions made for the analysis are: each soil layer is homogeneous, horizontal and the column extends to infinity, ground surface is leveled, and the incident earthquake motions propagate vertically. The nonlinear effect of the soil/sediment is approximated by modifying the linear elastic properties of the soil based on the induced strain level. Further, the strain compatible shear modulus and damping ratio values are iteratively calculated to generate the transfer function for each soil layer. This transfer function is convolved with the Fourier series of the input (bedrock) motion to generate the Fourier series of the output motion at ground surface thus delivering peak ground acceleration, acceleration time history, stress-strain time history, response spectra and amplification spectra at each site of interest (detailed theory and algorithm is given in Chapter 8).

For the present investigation, stochastically simulated synthetic ground motions of the four earthquakes which have affected the region most *viz.* the 1897 Shillong earthquake of  $M_w$  8.1, the 1918 Srimangal earthquake of  $M_w$  7.6, the Dhubri earthquake of  $M_w$  7.1 and the 1934 Bihar-Nepal earthquake of  $M_w$  8.1 have been used by inheriting the earthquake parameters from Nath *et al.* (2014) (described in Chapter 8 in Table 8.1) and an initial estimate of 5% damping has been considered for all soil types to perform the dynamic analysis. The amplification spectrum thus obtained at various locations of Kolkata for these four earthquakes have been averaged out to provide the highest value  $\pm$ one standard deviation of site amplification factor at predominant frequency for the corresponding location. The average amplification spectrum and the corresponding standard deviation curves for Saltlake, Kolkata along with the corresponding ground motions at both the engineering bedrock and the earth's surface are shown in Figure 10.1.

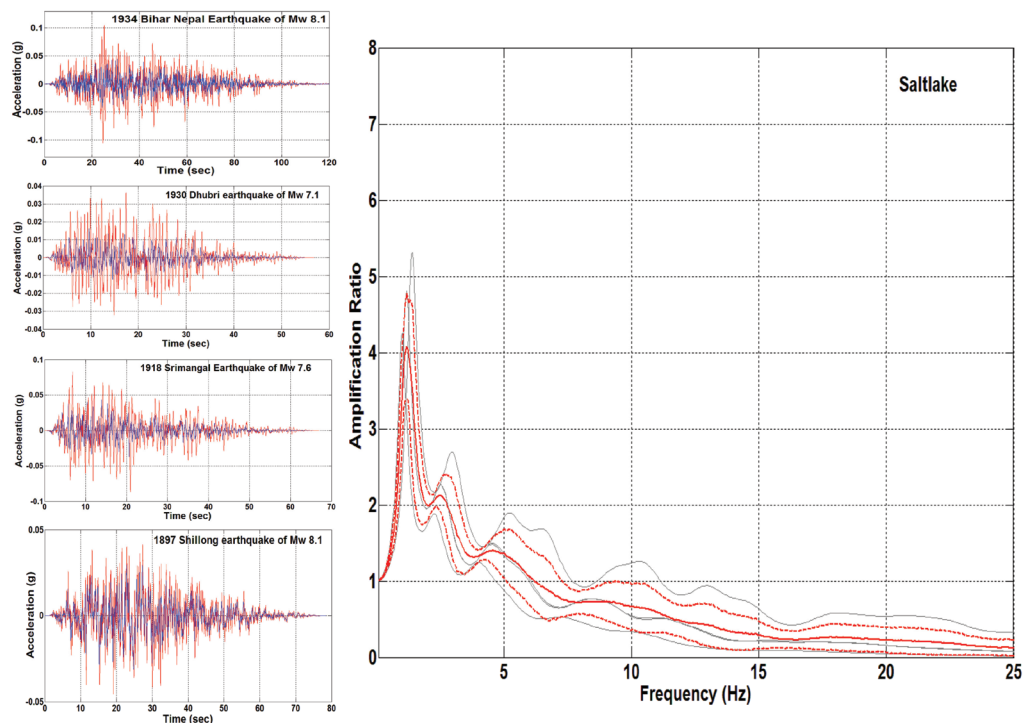
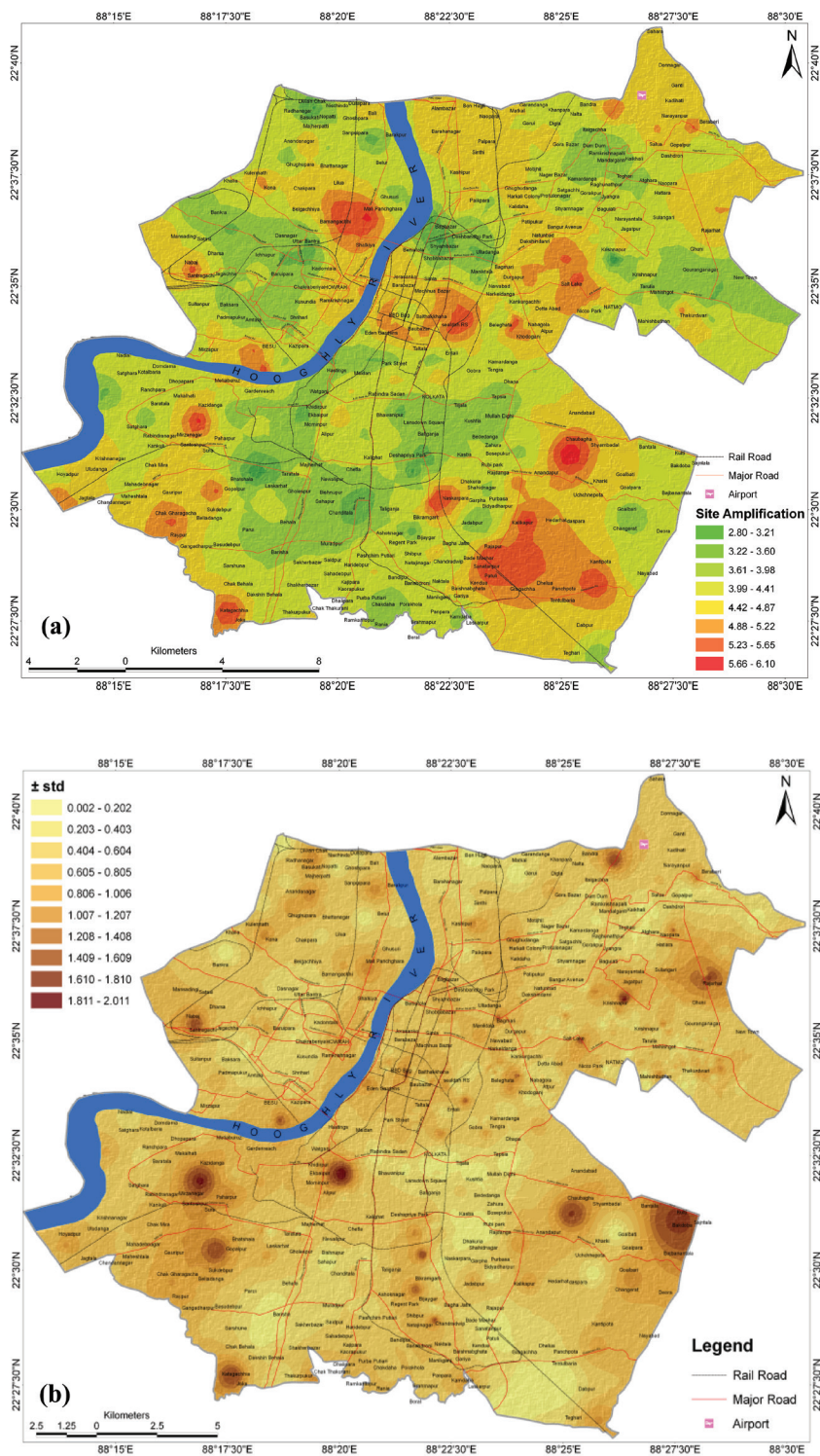


Figure 10.1

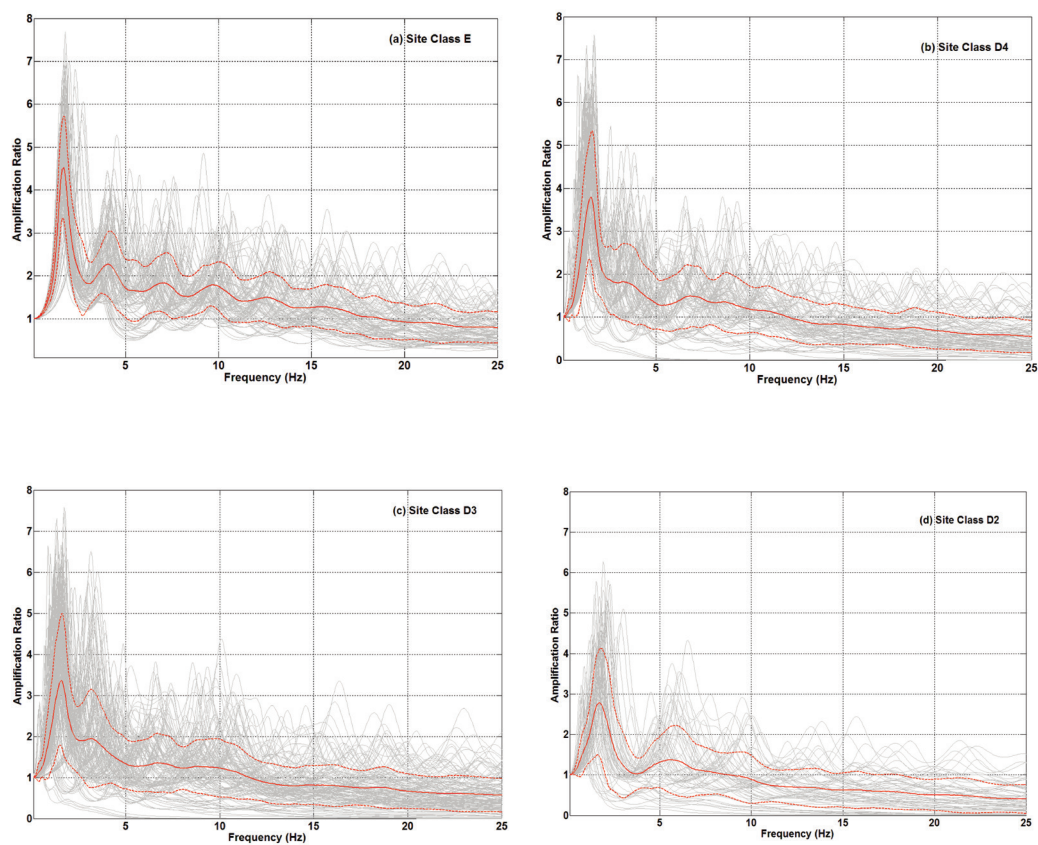
The Amplification Spectra at Saltlake (Bold red color) along with the associated  $\pm$  standard deviations (dotted red color) obtained by averaging the amplification spectra of the four considered earthquakes *viz.* the 1897 Shillong earthquake of  $M_w$  8.1, the 1918 Srimangal earthquake of  $M_w$  7.6, the Dhubri earthquake of  $M_w$  7.1, and the 1934 Bihar-Nepal earthquake of  $M_w$  8.1 and the respective ground motions.

1-D shear wave velocity profile at each of 1957 locations defined by calibrating 654 borehole site information with 85 location MASW based surface measurements, 1200 location microtremor recordings and 18 downhole refraction survey in the City have been subjected to both these near- and far-field earthquake ground motions wherein site amplification factor at the predominant frequency is quantified at each site in question. These site amplification factors on GIS platform are interpolated through Inverse Distance Weighted (IDW) means via geological and geomorphological control. The Site Amplification map thus obtained for Kolkata depicted in Figure 10.2(a) reveals a variation in the range of 2.8–6.1 with the associated error map of  $\pm$  standard deviation distribution given in Figure 10.2(b).



**Figure 10.2** (a) Spatial distribution of Site Amplification in Kolkata depicting the dominance of the values in the range of 3.61-4.41, and (b) The associated error map in terms of ± standard deviation distribution.

The site amplification spectrum derived by considering both the near- and far-field aforesaid earthquakes for the sites falling in each of the site classes E, D4, D3, D2 & D1 are amalgamated and averaged out with in  $\pm$ one standard deviation to provide a generic site amplification spectra for each site classes as shown in Figure 10.3. Thereafter, the site amplification factor is obtained from the generic site amplification spectra for each site at the predominant frequency. The grey curves represent a composite of site amplification spectra associated with each site class for the said earthquakes while bold red curve represent the generic site amplification of the corresponding site class as an average spectrum and dotted red curves are associated  $\pm$ one standard deviation. It is evident from Figure 10.3 the higher site amplification factor of 4.5 has been found to be associated with very soft sediments of site class E followed by site class D4, D3, D2 and D1 with the average site amplification factor of 3.9, 3.4, 2.8 and 2.3 respectively.



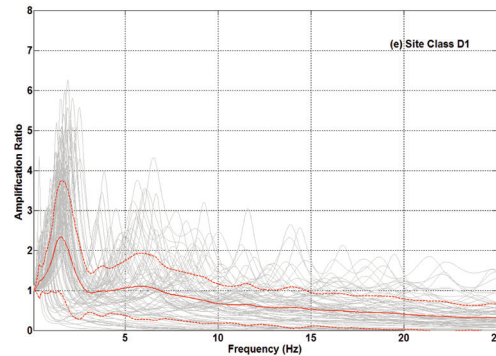


Figure 10.3

Generic Site Amplification Curves derived by considering four earthquakes *viz.* the 1897 Shillong earthquake of  $M_w$  8.1, the 1918 Srimangal earthquake of  $M_w$  7.6, the Dhubri earthquake of  $M_w$  7.1 and the 1934 Bihar-Nepal earthquake of  $M_w$  8.1 for (a) Site Class E, (b) Site Class D4, (c) Site Class D3, (d) Site Class D2, and (e) Site Class D1. Grey curves represent a composite of site amplification spectra associated with each site class. Bold red curve represent the generic site amplification of the corresponding site class as an average spectrum, while, dotted red curves are associated  $\pm$  one standard deviation.

### 10.3 Predominant Frequency

The local soil conditions may exhibit different fundamental frequencies depending on the sediment thickness and its physical properties (Nath and Thingbaijam, 2011b). The proximity of fundamental frequency of the sediment layer and the natural frequency of the buildings on which those are located indicate higher vulnerability owing to resonance effects which necessitates its assessment for mitigation purposes (Navarro and Oliveiram, 2006; Nath, 2011). In the present investigation the horizontal-to-vertical spectral ratio (HVSr) obtained from Nakamura method (Nakamura, 2000) at each of the 1200 microtremor survey sites provided predominant frequencies at those sites. Out of these 1200 sites, the 654 sites are selected which are in the proximity of the 654 borehole location where predominant frequency of the soil column have been obtained using two sets of data, one by Nakamura Ratio and another through DEEPSOIL analysis. Both of them are now segregated as per the site classes and for each site class a comparison analysis has been done between the clustered Nakamura location and the nearest borehole location and a 1:1 correspondence has also been obtained which gives a better control on predominant frequency distribution as depicted in Figure 10.4. The terrain is dominated by Site Class D4 ( $V_s^{30}$ : 240-180 m/s) with majority of predominant frequencies in the range of 1.0-2.25 Hz. On the other hand, Site Class D3 ( $V_s^{30}$ : 280-240 m/s) is mainly governed with the predominant frequencies in the range of 1.2-2.5 Hz. The predominant frequency for Site Class D2 ( $V_s^{30}$ : 320-280 m/s) lies in the range of 1.4-3.9 Hz, on the other hand, Site Class D1 ( $V_s^{30}$ : 360-320 m/s) has predominant frequencies in the range of 1.9-4.42 Hz. The lowest predominant frequency range of 0.6-1.7 Hz has been found to be associated with Site Class E.

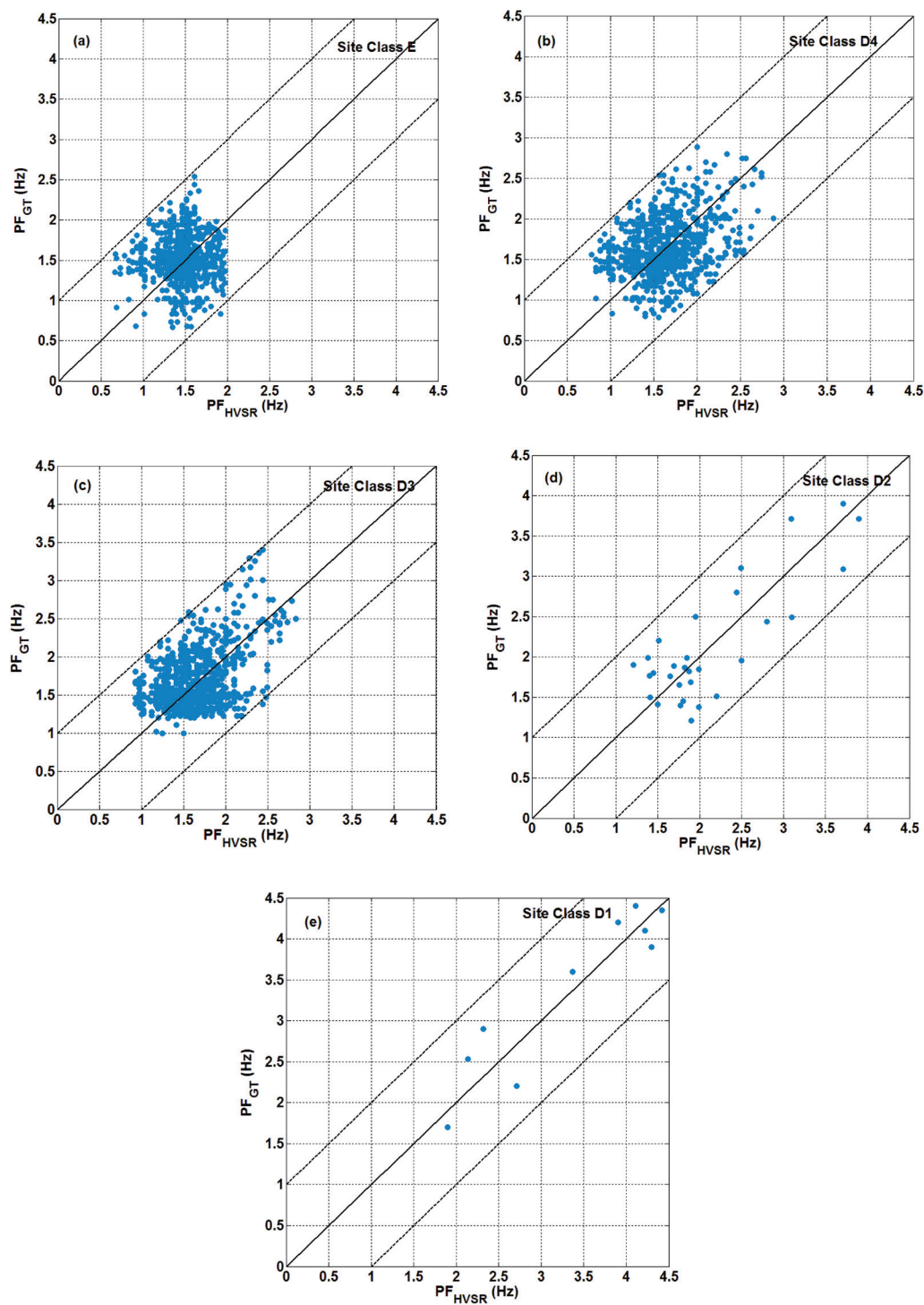
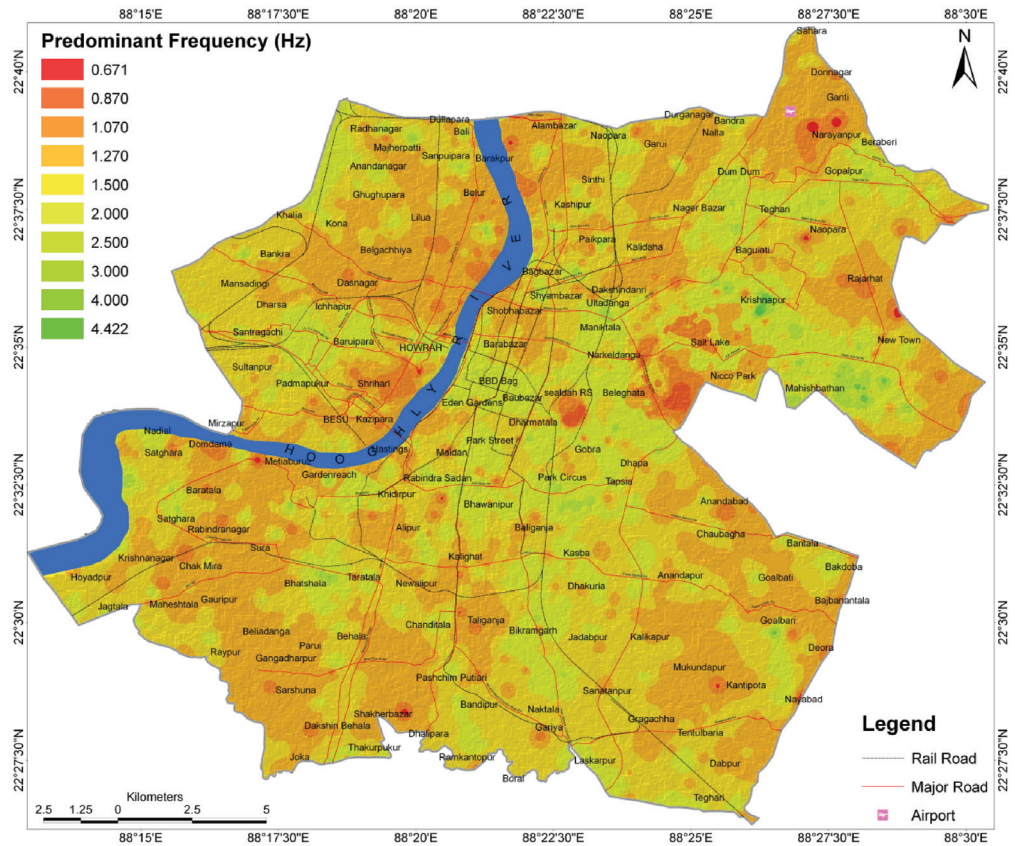


Figure 10.4

A site specific comparison between the predominant frequencies obtained by performing one dimensional equivalent linear site response analysis ( $PF_{GT}$ ) with those obtained from HVSR curves ( $PF_{HVSR}$ ) for (a) Site Class E, (b) Site Class D4, (c) Site Class D3, (d) Site Class D2, and (e) Site Class D1.

A predominant frequency distribution map for the City has been generated by interpolating the hybridized predominant frequencies at 1872 locations (1200 microtremor and 654 borehole sites) through Inverse Distance Weighted means via geological, geomorphological and site class control on GIS platform as shown in Figure 10.5 which shows a variation in the range of 0.67-4.42 Hz. The low predominant frequency is found to be associated with parts of Rajarhat, Saltlake, Dum Dum, Liluah, Shibpur region.



**Figure 10.5**

Spatial distribution of Predominant Frequency in Kolkata as obtained from HVSR curves of 1200 locations and by performing one dimensional equivalent linear site response analysis at 654 borehole sites.

## 10.4 Soil Liquefaction Assessment

Kolkata resides on deltaic flat land comprising of soft alluvial deposits belonging to Holocene-Pleistocene age which under favorable lithostratigraphic, geomorphological and ground water conditions exhibit liquefaction in sediments at varying depths of 5-15 m below the surface. Iwasaki *et al.* (1978; 1982) introduced Liquefaction Potential Index (LPI) in order to estimate the severity

of liquefaction for the upper 20 m soil column of a specific borehole location. The liquefaction susceptibility map of Kolkata due to 1934 Bihar-Nepal earthquake of  $M_w$  8.1 has been created by spatially distributing the LPI values on GIS platform presented in Figure 10.6 classifying the terrain into severely susceptible ( $LPI > 15$ ), highly susceptible ( $5 < LPI \leq 15$ ), moderately susceptible ( $LPI \leq 5$ ), and low susceptible ( $LPI = 0$ ) zones. The areas that have experienced damages due to 1934 Bihar-Nepal earthquake were found to exist within the Moderate and High susceptibility zones.

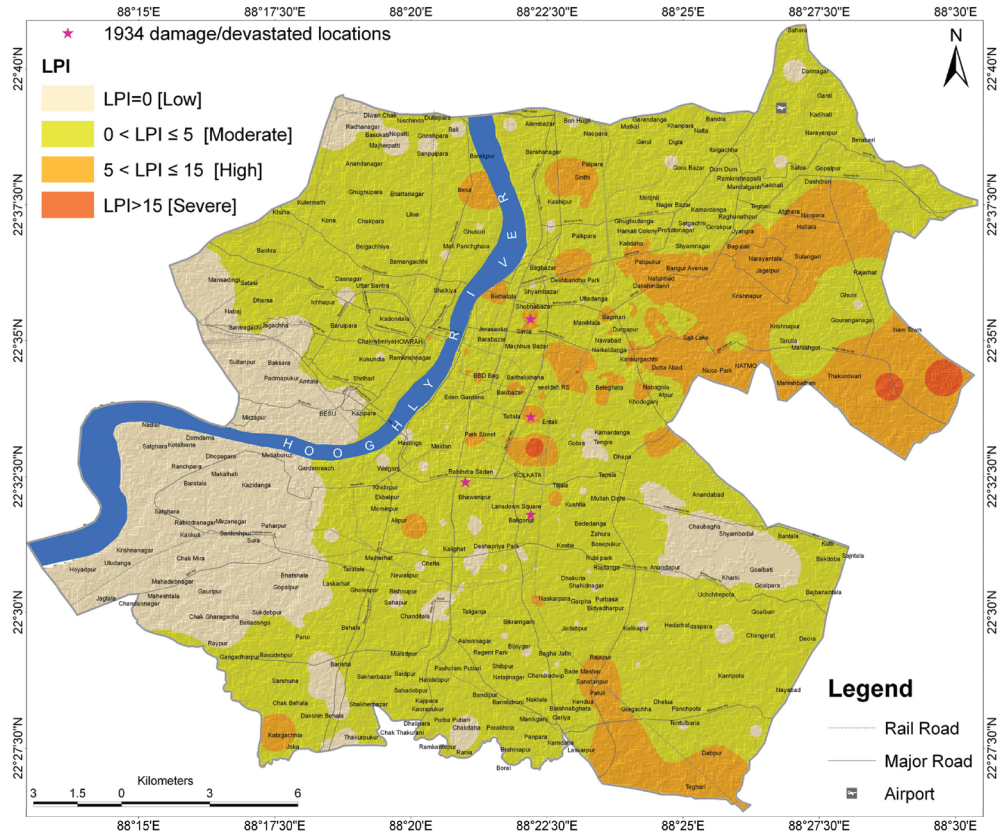


Figure 10.6

Liquefaction Susceptibility Map of Kolkata due to 1934 Bihar-Nepal earthquake of  $M_w$  8.1 prepared by spatially distributing Liquefaction Potential Index (LPI) values. An  $LPI > 15$  indicates a severe liquefaction hazard condition, an LPI between 5 and 15 indicates a tendency to liquefy, and  $LPI < 5$  depicts moderate to low liquefaction hazard condition. All the reported damage sites due to 1934 Bihar-Nepal earthquake of  $M_w$  8.1, marked as '★' falls in Moderate and High Liquefaction Zone.

The detailed liquefaction analysis performed at 654 borehole locations indicates the vulnerability of sediment layer of varying thickness lying in the depth range of 5-15 m below ground surface under the influence of intense ground shaking due to high PGA. The presence of non-plastic sand and sandy silt in conjunction with the shallow ground water table has enhanced the hazard due to liquefaction for the aforementioned depth range below the ground level.

## 10.5 Site Categorization of Kolkata – A Relook

The effective shear wave velocity ( $V_s^{30}$ ) for a site act as a good indicator of shallow subsurface condition and is directly related to the sediment stiffness thus its spatial distribution helps in delineating the presence of soft sediments in the terrain which makes it an effective proxy to perform site classification (Aki and Richards, 2002). NEHRP has recommended five site classes based on  $V_s^{30}$  with similar site response (Nath and Thingbaijam, 2011b) viz. site class A and site class B with  $V_s^{30} \geq 1500$  m/s &  $1500 \geq V_s^{30} > 760$  m/s respectively are assigned with hard rock and rock site conditions, whereas, site class C with  $760 > V_s^{30} \geq 360$  m/s corresponds to soft rock, hard or very stiff soils or gravels while, stiff soils with  $360 > V_s^{30} \geq 180$  m/s designates site class D. On the other hand, Sun (2004) has proposed subclasses in site class C and D which not only considers effective shear wave velocity  $V_s^{30}$  distribution but also the corresponding site periods, thus subdividing Site Class D into four subcategories: D1 ( $V_s^{30}$ : 360-320 m/s;  $T_G$ : 0.27-0.34 sec), D2 ( $V_s^{30}$ : 320-280 m/s;  $T_G$ : 0.34-0.43 sec), D3 ( $V_s^{30}$ : 280-240 m/s;  $T_G$ : 0.43-0.55 sec), and D4 ( $V_s^{30}$ : 240-180 m/s;  $T_G$ : 0.55-0.68 sec). However, very soft sediments with  $V_s^{30} < 180$  implicates site class E which may get upgraded in site class F provided any of the following conditions (Nath and Thingbaijam, 2011b):

- i) Soils vulnerable to potential failure or collapse under seismic loading such as liquefiable soil, quick and highly sensitive clays, and collapsible weakly cemented soils,
- ii) Peats and/or highly organic clay (soil thickness  $> 3$  m),
- iii) Very high plastic clays (soil thickness  $> 8$  m with  $PI > 75$ ), and
- iv) Very thick soft/medium clays (soil thickness  $> 36$  m).

The Site Classification map of Kolkata has been generated by using 1-D  $V_s$  profiles at 1957 locations obtained from 654 geotechnical borehole sites, 85 MASW sites, 1200 microtremor survey locations and 18 insitu downhole seismic survey sites, considering both the NEHRP and Sun (2004) site classification nomenclature, shown in Figure 10.7, which exhibits the presence of Site Class E, D4, D3, D2 & D1 with the dominance of Site Classes corresponding to low shear wave velocity viz. D4 followed by Site Class D3 and Site Class E in the region which may be attributed to the presence of a low velocity layer of high plastic silty clay associated with decomposed wood/peat. Site Class E marks its presence in parts of the city at Howrah, Shibpur, Saltlake, Nicco Park, Dhapa, Jadavpur and so on.

However, the presence of soft liquefaction prone alluvial sediments in Kolkata has necessitated the reclassification of the terrain by introducing site class F. Owing to the highest damage reporting due to the 1934 Bihar-Nepal earthquake of  $M_w$  8.1 in the terrain among all the past earthquakes affecting the City, the liquefaction scenario for this earthquake has been considered to reclassify the terrain by upgrading few patches of site class E which are expected to undergo liquefaction related damages into site class F, as depicted in Figure 10.7. The patches of site class F have been identified in northeastern regions encompassing Saltlake, outskirts of Rajarhat & New Town *etc.* Two small patches of site class F have also been identified in southeastern region. The regions

associated with site class F are found to be underlain by very soft sediments with low SPT-N values and shallow ground water table in the depth range of 0.5-2.0 m.

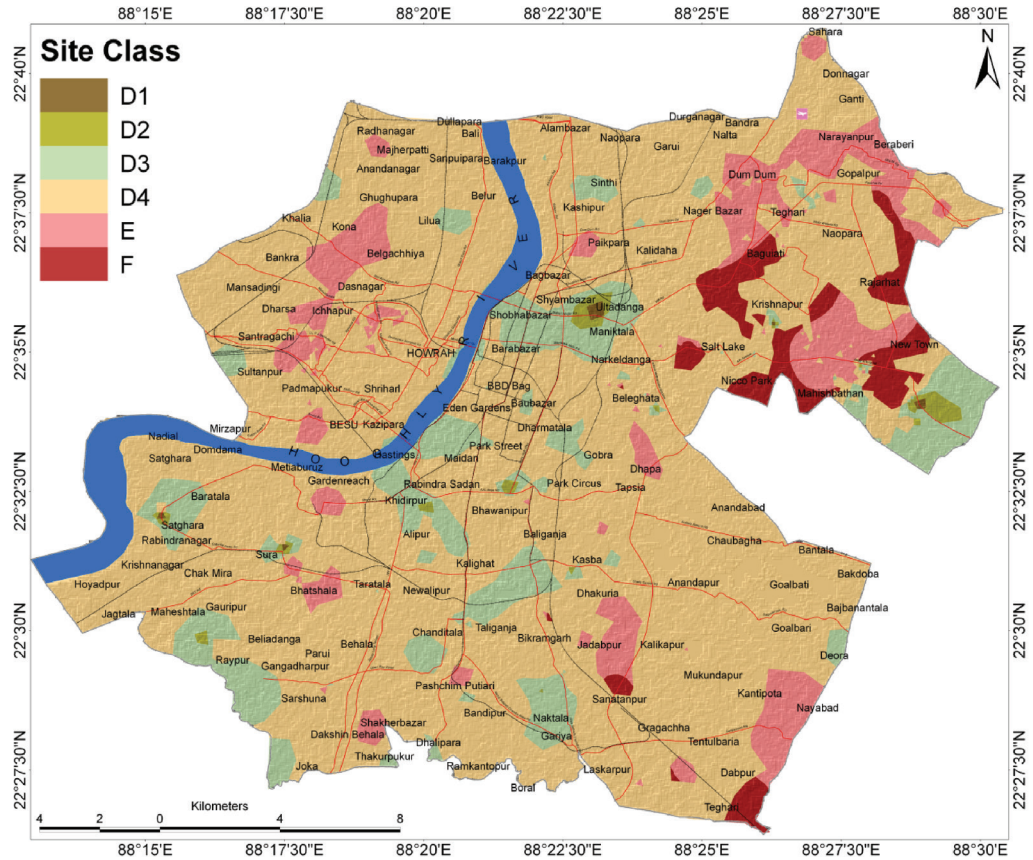


Figure 10.7

Site Classification map of Kolkata adhering Sun (2004), Sun and Shin (2009) & Sun *et al.* (2009) and displaying the presence of Site Class E, D4, D3, D2 & D1 in the terrain with the dominance of Site Class D4 followed by Site Class D3 and Site Class E in the region. Site class F has also marked its presence in the region.

## 10.6 Site Coefficients

Site coefficient is defined as the ratio of the spectral acceleration at site with that of reference rock outcrop at the same period (Borcherdt, 1996; Dobry *et al.*, 1999, Sun *et al.*, 2005). The site coefficients that are used to characterize local site amplification are divided into short-period amplification factor,  $F_a$  for 0.1-0.5 sec and mid-period amplification factor,  $F_v$  for 0.4-2.0 sec (NEHRP, Aboye *et al.*, 2014; Sun *et al.*, 2008; Sun *et al.*, 2005; Borcherdt, 1994). Owing to the dependence of site effects on the local subsurface conditions (Seed *et al.*, 1976), region specific estimation of the site amplification factors will be more reliable for a soft alluvial terrain like

Kolkata. Therefore, site coefficients  $F_a$  &  $F_v$  for the City have been estimated by using the response spectra of both the soil and rock sites corresponding to the four major earthquakes which have affected the City most viz. the 1897 Shillong earthquake of  $M_w$  8.1, the 1918 Srimangal earthquake of  $M_w$  7.6, the Dhubri earthquake of  $M_w$  7.1 and the 1934 Bihar-Nepal earthquake of  $M_w$  8.1 at each of 654 borehole locations, by using the following formulations (Sun *et al.*, 2005)

$$F_a = \frac{R_{soil}}{R_{rock}} \frac{1}{0.4} \int_{0.1}^{0.5} \frac{RS_{soil}(T)}{RS_{rock}(T)} dT \quad (10.1)$$

$$F_v = \frac{R_{soil}}{R_{rock}} \frac{1}{1.6} \int_{0.4}^{2.0} \frac{RS_{soil}(T)}{RS_{rock}(T)} dT \quad (10.2)$$

where  $RS_{soil}$  and  $RS_{rock}$  are response spectra on soil and rock at a given period  $T$ , whereas,  $R_{soil}$  and  $R_{rock}$  are the hypocentral distances of soil and rock sites respectively.

The subsurface conditions and stiffness of sediments underlying a site can be quantified in terms of its effective shear wave velocity ( $V_s^{30}$ ), lower the  $V_s^{30}$  softer will be the sediments, higher will be the site amplification and lower will be the predominant frequency & vice-versa. Therefore, a nonlinear regression has been performed between the set of site coefficients viz.  $F_a$  and  $F_v$  calculated from the response spectra of the aforesaid earthquakes and their corresponding  $V_s^{30}$  for the five site classes identified in the terrain as shown in Figures 10.8 to 10.12. The site amplification factors are found to be increasing with decrease in effective shear wave velocity ( $V_s^{30}$ ) i.e. Site Class E/~F exhibited highest  $F_a$  and  $F_v$  values followed by Site Classes D4, D3, D2 and D1.

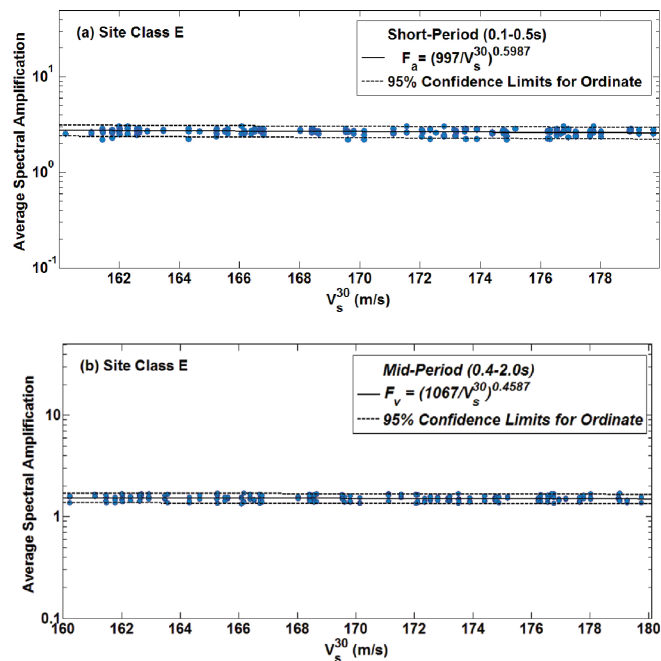


Figure 10.8

Regression curves between average spectral amplification and effective shear wave velocity,  $V_s^{30}$  (bold black curve) superimposed with the 95% confidence intervals for the ordinates to the true population regression line (dotted black curves) corresponding to Site Class E ( $V_s^{30} < 180$  m/s) for (a) Short-Period,  $F_a$  (0.1-0.5 sec), and (b) Mid-Period,  $F_v$  (0.4-2.0 sec).

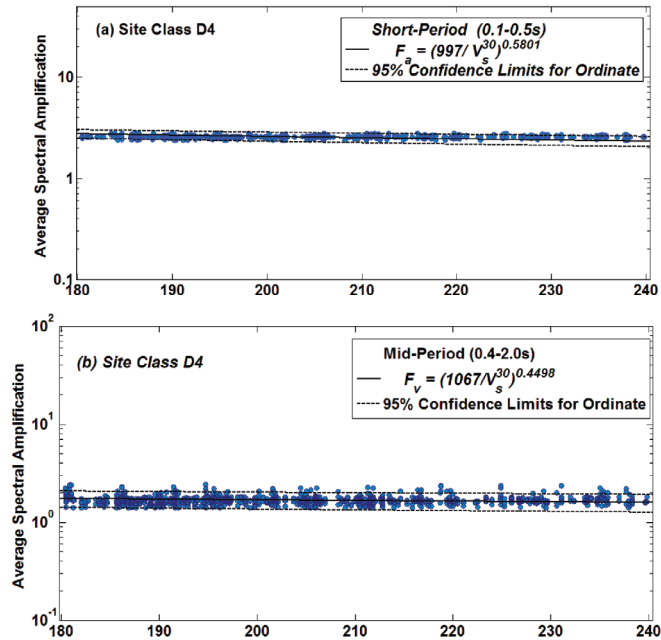


Figure 10.9

Regression curves between average spectral amplification and effective shear wave velocity,  $V_s^{30}$  (bold black curve) superimposed with the 95% confidence intervals for the ordinates to the true population regression line (dotted black curves) corresponding to Site Class D4 ( $180 \leq V_s^{30} < 240$  m/s) for (a) Short-Period,  $F_a$  (0.1-0.5 sec), and (b) Mid-Period,  $F_v$  (0.4-2.0 sec).

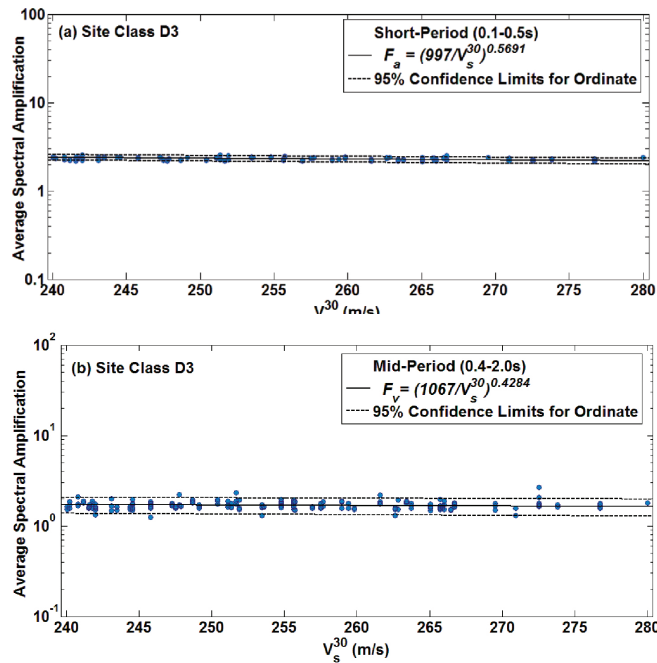


Figure 10.10

Regression curves between average spectral amplification and effective shear wave velocity,  $V_s^{30}$  (bold black curve) superimposed with the 95% confidence intervals for the ordinates to the true population regression line (dotted black curves) corresponding to Site Class D3 ( $240 \leq V_s^{30} < 280$  m/s) for (a) Short-Period,  $F_a$  (0.1-0.5 sec), and (b) Mid-Period,  $F_v$  (0.4-2.0 sec).

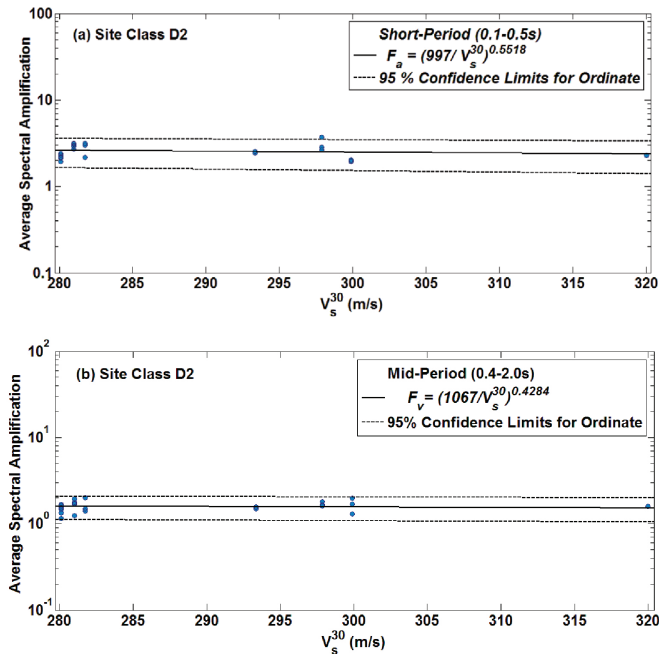


Figure 10.11

Regression curves between average spectral amplification and effective shear wave velocity,  $V_s^{30}$  (bold black curve) superimposed with the 95% confidence intervals for the ordinates to the true population regression line (dotted black curves) corresponding to Site Class D2 ( $280 \leq V_s^{30} < 320$  m/s) for (a) Short-Period,  $F_a$  (0.1-0.5 sec), and (b) Mid-Period,  $F_v$  (0.4-2.0 sec).

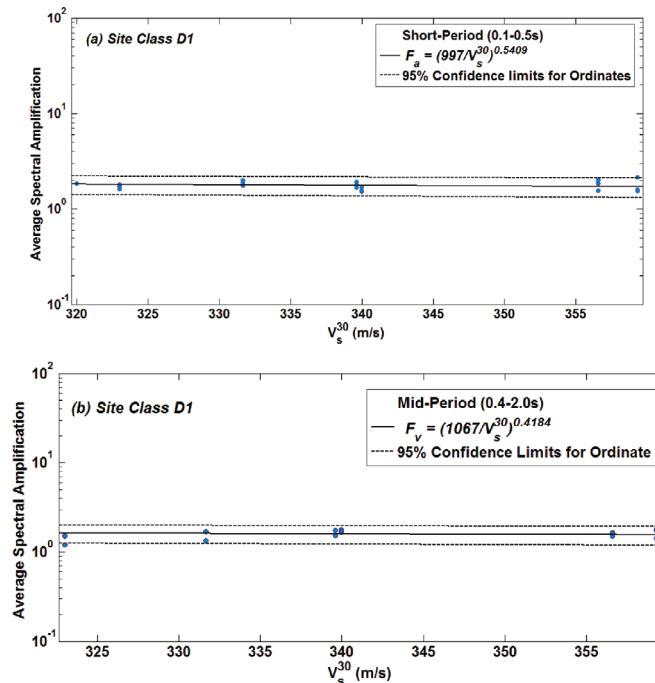


Figure 10.12

Regression curves between average spectral amplification and effective shear wave velocity,  $V_s^{30}$  (bold black curve) superimposed with the 95% confidence intervals for the ordinates to the true population regression line (dotted black curves) corresponding to Site Class D1 ( $320 \leq V_s^{30} < 360$  m/s) for (a) Short-Period,  $F_a$  (0.1-0.5 sec), and (b) Mid-Period,  $F_v$  (0.4-2.0 sec).

Table 10.1

Site class specific nonlinear regression equations between average spectral amplification and effective shear wave velocity for Short-Period,  $F_a$  (0.1-0.5 sec)

Site Class	$V_s^{30}$ (m/s)	Site Amplification Factor For Short-period (0.1-0.5 sec), $F_a$	Nonlinear relation between Short-Period (0.1-0.5 sec), $F_a$ and $V_s^{30}$
Site Class D1	360-320	<1.87	$F_a = (997/V_s^{30})^{0.5409}$
Site Class D2	320-280	2.06-1.87	$F_a = (997/V_s^{30})^{0.5518}$
Site Class D3	280-240	2.28-2.06	$F_a = (997/V_s^{30})^{0.5691}$
Site Class D4	240-180	2.78-2.28	$F_a = (997/V_s^{30})^{0.5801}$
Site Class E/~F	<180	>2.78	$F_a = (997/V_s^{30})^{0.5987}$

Table 10.2

Site class specific nonlinear regression equations between average spectral amplification and effective shear wave velocity for Mid-Period,  $F_v$  (0.4-2.0 sec)

Site Class	$V_s^{30}$ (m/s)	Site Amplification Factor For Mid-period (0.4-2.0 sec), $F_v$	Nonlinear relation between Mid-Period (0.4-2.0 sec), $F_v$ and $V_s^{30}$
Site Class D1	360-320	<1.67	$F_v = (1067/V_s^{30})^{0.4184}$
Site Class D2	320-280	1.79-1.67	$F_v = (1067/V_s^{30})^{0.4284}$
Site Class D3	280-240	1.95-1.79	$F_v = (1067/V_s^{30})^{0.4376}$
Site Class D4	240-180	2.26-1.95	$F_v = (1067/V_s^{30})^{0.4498}$
Site Class E/~F	<180	>2.26	$F_v = (1067/V_s^{30})^{0.4587}$

## 10.7 Concluding Remarks

Site conditions have a significant influence on the seismic hazard potential of a region and therefore, its characterization has emerged as a crucial step in the quantification of seismic hazard associated with high risk urban centers across the globe (Nath and Thingbaijam, 2009; 2011b). The present study appraises a site specific seismic response analysis for the thick alluvial terrain of Kolkata in terms of predominant frequency, site amplification and site coefficients *viz.*  $F_a$  (0.1-0.5 sec) &  $F_v$  (0.4-2.0 sec) based on the enriched geological, geomorphological, geotechnical and geophysical database of the region. Additionally a site class based generic study of the said attributes reveal that the soft sediments associated with low  $V_s^{30}$  and high  $T_G$  exhibits low predominant frequency and high site amplification *e.g.* site class E/~F ( $V_s^{30}$  < 180 m/s;  $T_G$  > 0.68 sec) shows lowest predominant frequencies within the range of 0.6-1.7 Hz and higher site amplification of 4.5. In contrast the site class D1 ( $V_s^{30}$ : 360-320 m/s;  $T_G$ : 0.27-0.34 sec) exhibits higher predominant frequency in the range of 1.9-4.42 Hz and lower site amplification value of 2.3. The high site amplification

may be attributed to the presence of filled up coarse grained sand/silty sand deposits, shallow water table depth which lead to lowering of SPT-N values and association with low effective shear wave velocities. A site-specific soil liquefaction analysis exhibits the vulnerability of the sediments underlying parts of northeastern and southeastern regions encompassing Saltlake, outskirts of Rajarhat & New Town *etc.* and facilitated reclassification of site class E to site class F at those locations wherever liquefaction is exhibited other attributes remaining the same. These site attributes are finally adopted in the seismic hazard microzonation considering both the seismological and geohazard regimes, site condition being grouped in the later while site amplification and predominant frequency fall in the former. Site coefficient is the most essential parameter that defines the seismic coefficient in conjunction with the zone factor and other important design parameters including design response spectra.